National Conference with International Participation
ENGINEERING MECHANICS 2007
Svratka, Czech Republic, May 14 – 17, 2007

HIGH ORDER GEOMETRICAL AND FUNCTIONAL DISCRETIZATION FOR THE NAVIER–STOKES EQUATIONS

B. Horeni*, Z. Chara *

Summary: *The accuracy of numerical solution of fluid dynamic tasks depends on both the geometrical and functional discretization. The paper deals with an applicability of high order methods for geometrical as well as functional approximations. Usefulness of this approach is demonstrated on selected examples.*

Geometrical discretization

Geometrical discretization using the linear elements (with the straight edges in 2D geometry or the planar faces in 3D one) subjects to some restrictions. A dense mesh is required in a neighborhood of the curved walls even if a solution is considerably smooth. The smoothly curved walls can be modeled with the straight edges (2D case) or the planar faces (3D case) with second–order accuracy. To improve the accuracy, a high order approximation of the curved walls is required.

We now use the mapping of plane u, v to plane x, y in the form

$$\boldsymbol{r}(x,y) = \boldsymbol{R}\,\boldsymbol{m} = \sum_i \boldsymbol{r}_i u^{p_i} v^{q_i} = \boldsymbol{r}_0 + \boldsymbol{r}_1 u + \boldsymbol{r}_2 v + \boldsymbol{r}_3 uv + \dots\,, \tag{1}$$

where $\boldsymbol{R}$ is a set of constant vectors

$$\boldsymbol{R} = [\boldsymbol{r}_0, \boldsymbol{r}_1, \boldsymbol{r}_2, \boldsymbol{r}_3, \dots]\,. \tag{2}$$

Jacobian is given by

$$\begin{aligned} D = (\partial\boldsymbol{r}/\partial u \times \partial\boldsymbol{r}/\partial v) \circ \boldsymbol{k} &= [\partial\boldsymbol{r}/\partial u, \partial\boldsymbol{r}/\partial v] \\ &= \sum_{i,j} [\boldsymbol{r}_i, \boldsymbol{r}_j]\; p_i q_j u^{(p_i+p_j-1)} v^{(q_i+q_j-1)}\,. \end{aligned} \tag{3}$$

*Institute of Hydrodynamics Academy of Sciences of the Czech Republic, Pod Patankou 5, 16612 Prague 6, Czech Republic

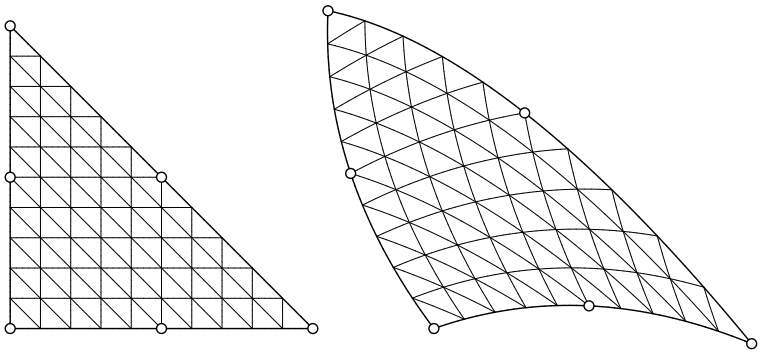

Figure 1: Quadratic mapping of a standard triangle.

With a simple algorithm it is possible to rewrite the Jacobian to the form

$$D = \boldsymbol{D}\,\boldsymbol{m} = D_0 + D_1 u + D_2 v + D_3 uv + \ldots + D_i u^{p_i} v^{q_i} + \ldots \,. \tag{4}$$

For a linear mapping it follows that

$$\boldsymbol{r}(x,y) = \boldsymbol{r}_0 + \boldsymbol{r}_1 u + \boldsymbol{r}_2 v \,, \tag{5}$$

the Jacobian is a simple scalar constant D_0

$$D = D_0 = (\boldsymbol{r}_1 \times \boldsymbol{r}_2) \circ \boldsymbol{k} = [\boldsymbol{r}_1, \boldsymbol{r}_2] \,. \tag{6}$$

For a quadratic mapping (Fig.1)

$$\boldsymbol{r}(x,y) = \boldsymbol{r}_0 + \boldsymbol{r}_1 u + \boldsymbol{r}_2 v + \boldsymbol{r}_3 uv + \boldsymbol{r}_4 u^2 + \boldsymbol{r}_5 v^2 \tag{7}$$

we obtain

$$D = D_0 + D_1 u + D_2 v + D_3 uv + D_4 u^2 + D_5 v^2 \,, \tag{8}$$

where

$$\begin{aligned} D_0 &= [\boldsymbol{r}_1, \boldsymbol{r}_2] \,, \\ D_1 &= [\boldsymbol{r}_1, \boldsymbol{r}_3] + 2\,[\boldsymbol{r}_4, \boldsymbol{r}_2] \,, \\ D_2 &= 2\,[\boldsymbol{r}_1, \boldsymbol{r}_5] + [\boldsymbol{r}_3, \boldsymbol{r}_2] \,, \\ D_3 &= 4\,[\boldsymbol{r}_4, \boldsymbol{r}_5] \,, \\ D_4 &= 2\,[\boldsymbol{r}_4, \boldsymbol{r}_3] \,, \\ D_5 &= 2\,[\boldsymbol{r}_3, \boldsymbol{r}_5] \,. \end{aligned} \tag{9}$$

Mapping of an order n has $(n+1)(n+2)/2$ coefficients and its corresponding Jacobian $n(2n-1)$ coefficients. Some restricted mappings are useful. For example a bilinear mapping $\boldsymbol{r}(x,y) = \boldsymbol{r}_0 + \boldsymbol{r}_1 u + \boldsymbol{r}_2 v + \boldsymbol{r}_3 uv$ transforms a standard triangle with vertices $(0,0)$, $(1,0)$ and $(0,1)$ to a common triangle with two straight edges and one curvilinear edge, or unit square with vertices $(0,0)$, $(1,0)$, $(1,1)$ and $(0,1)$ to a common quadrilateral.

Functional discretization

The increasing of a polynomial degree of functional discretization improves the quality of the smooth solution. Using an orthogonal basis will leave out an inversion of the mass matrix. Another, perhaps more important, advantage, is that an orthogonal basis makes the modification of a polynomial degree trivial [17]. In the following a process, how to sequentially introduce a set of monomials $u^p v^q$ into an orthonormal basis will be described. We use set of monomials

$$\boldsymbol{m} = [1, u, v, uv, u^2, v^2, u^2 v, uv^2, u^3, v^3 \ldots u^{p_i} v^{q_i} \ldots]^T . \tag{10}$$

To generate a sequence of orthonormal polynomials from the generating set of monomials $u^p v^q$ we use an algorithm equivalent to the Gram–Schmidt process which transforms a given set of n input vectors $\boldsymbol{a}_i, i = 1, \ldots, n$ to a set of n orthonormal vectors $\boldsymbol{e}_i$ spanning the same vector space. The procedure is outlined in an algorithm

1. $\boldsymbol{e}_1 \leftarrow \boldsymbol{a}_1 / ||\boldsymbol{a}_1||$
2. For $i = 2, \ldots, n$
   (a) $\boldsymbol{a}_i \leftarrow \boldsymbol{a}_i - \sum_{j=1}^{i-1} (\boldsymbol{a}_i, \boldsymbol{e}_j)\, \boldsymbol{e}_j$
   (b) $\boldsymbol{e}_i \leftarrow \boldsymbol{a}_i / ||\boldsymbol{a}_i||$

In step 2a of this algorithm, the i–th input vector is replaced by its orthogonal component to a vector space spanned by the first $i-1$ orthonormal vectors, thus by the difference between a vector and its projection to a sub–space.

An equivalent procedure can be applied to polynomial functions on the canonical elements (unit square or standard triangle) to transform a given set of monomials m_i to a set of orthonormal polynoms E_i

1. $E_0 \leftarrow m_0 / ||m_0||$
2. For $i = 1, \ldots, n$
   (a) $E_i \leftarrow m_i - \sum_{j=0}^{i-1} (m_i, E_j)\, E_j$
   (b) $E_i \leftarrow E_i / ||E_i||$

If a mapping is linear, we can obtain a universal orthonormal basis, such as for any triangle with straight edges in the following form

$$\begin{aligned}
\sqrt{[\boldsymbol{r}_1, \boldsymbol{r}_2]}\, E_0 &= \sqrt{2}\,, \\
\sqrt{[\boldsymbol{r}_1, \boldsymbol{r}_2]}\, E_1 &= -2 + 6u\,, \\
\sqrt{[\boldsymbol{r}_1, \boldsymbol{r}_2]}\, E_2 &= 2\sqrt{3}\,(-1 + u + 2v)\,, \\
\sqrt{[\boldsymbol{r}_1, \boldsymbol{r}_2]}\, E_3 &= 3\sqrt{2/7}\,(1 - 4u - 4v + 20uv)\,, \ldots
\end{aligned} \tag{11}$$

where $[\boldsymbol{r}_1, \boldsymbol{r}_2]$ is a simple scalar constant , the Jacobian $D_0 = (\boldsymbol{r}_1 \times \boldsymbol{r}_2) \circ \boldsymbol{k} = [\boldsymbol{r}_1, \boldsymbol{r}_2]$.

For a nonlinear mapping of a canonical element we obtain unique set of orthonormal functions for each curvilinear element.

This is illustrated in Fig.2 where several functions E_i are shown (all functions are up to degree 5 except constant function E_0). It is clear that the high order methods enable to approximate the solution inside the element in much more detail.

Artificial compressibility method

Navier-Stokes equations of an unsteady flow of a compressible liquid are a system of mixed hyperbolic–parabolic type. For an incompressible liquid the equations form a system of elliptic–parabolic type. The primary difficulty in solving the incompressible flow in primitive variables stems from the lack of time derivative in continuity equation. Most of the methods require a solution of Poisson equation for coupling between the velocity and the pressure field in each step. This requirement is poorly satisfied in robust and effective numerical methods where balance of mass, momentum and energy are used. But there is a possibility how this disadvantage can be overcome.

The method is known as the artificial compressibility or pseudo–compressibility method and was first introduced in [6]. In this formulation a time derivative of pressure is added to the continuity equation. With the momentum equations we obtain a hyperbolic system with artificial pressure waves of finite speed which can be solved in pseudotime to divergence–free steady–state solution. As a consequence of this many of efficient and well developed compressible flow algorithms can be used for this method. Using subiteration in pseudotime can the method extended to solve time dependent problems [19, 2].

Following the artificial compressibility formulation, a time derivative of pressure p is added to the compressibility equation

$$\frac{\partial p}{\partial t} + \beta \left(\frac{\partial v_x}{\partial x} + \frac{\partial v_y}{\partial y} \right) = 0, \tag{12}$$

where β is known as the pseudo–compressibility constant which is linked with an artificial sound velocity a by the relation $\beta = 1/a^2$ [1].

The equations for incompressible viscous flow are presented here in nondimensional form for $\overline{x} = x/L$, $\overline{y} = y/L$, $\overline{v}_x = v_x/V_\infty$, $\overline{v}_y = v_y/V_\infty$, $\overline{p} = p/(\rho V_\infty^2)$, $\overline{t} = tV_\infty/L$, $M_\infty = V_\infty/a$ and $Re_\infty = V_\infty L/\nu_\infty$. Here t represents the pseudo–time and is not related to physical time. Combining the momentum equations for the incompressible Navier–Stokes equations with equation (12) results in system

$$\frac{\partial \boldsymbol{U}}{\partial t} + \frac{\partial \boldsymbol{F}_x}{\partial x} + \frac{\partial \boldsymbol{F}_y}{\partial y} = 0, \tag{13}$$

where $\boldsymbol{U}$ is vector of variables

$$\boldsymbol{U} = [\overline{p}, \overline{v}_x, \overline{v}_y]^T, \tag{14}$$

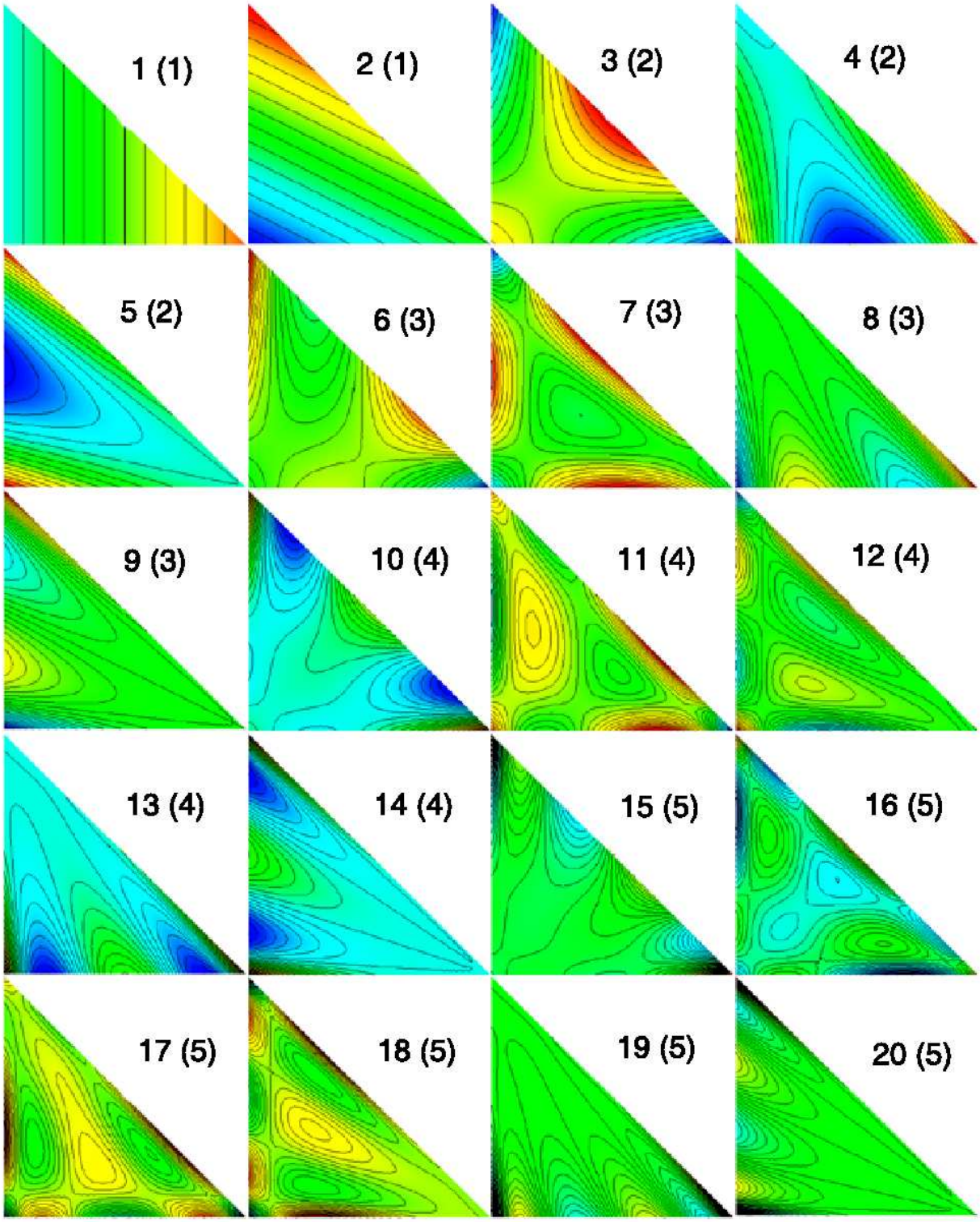

Figure 2: Orthonormal basis on a canonical triangle. In brackets is degree of orthonormal polynom.

Vectors of flow components in directions of co-ordinates $\boldsymbol{F}_x$ and $\boldsymbol{F}_y$ are

$$\boldsymbol{F}_x = \begin{bmatrix} \overline{v}_x/M_\infty^2 \\ \overline{v}_x^2 + \overline{p} - \overline{\tau}_{xx} \\ \overline{v}_x\overline{v}_y - \overline{\tau}_{xy} \end{bmatrix}, \qquad \boldsymbol{F}_y = \begin{bmatrix} \overline{v}_y/M_\infty^2 \\ \overline{v}_x\overline{v}_y - \overline{\tau}_{yx} \\ \overline{v}_y^2 + \overline{p} - \overline{\tau}_{yy} \end{bmatrix}, \tag{15}$$

and components of symetric shear stress tensor $\overline{\tau}$ are

$$\begin{array}{rcl} \overline{\tau}_{xx} & = & \frac{2}{3}\ \left(2\ \partial\overline{v}_x/\partial\overline{x} - \partial\overline{v}_y/\partial\overline{y}\right)/Re_\infty, \\ \overline{\tau}_{yy} & = & \frac{2}{3}\ \left(2\ \partial\overline{v}_y/\partial\overline{y} - \partial\overline{v}_x/\partial\overline{x}\right)/Re_\infty, \\ \overline{\tau}_{xy} & = & \left(\partial\overline{v}_x/\partial\overline{y} + \partial\overline{v}_y/\partial\overline{x}\right)/Re_\infty. \end{array} \tag{16}$$

To solve the equation (13) a discontinuous Galerkin method was used. The discontinuous Galerkin method is especially a highly compact formulation that provides a method for obtaining a high accuracy solution on the unstructured grids [12, 3]. Since solutions of the incompressible equations do not have strong discontinuities (shocks), it is possible solving without need for any limiting and high order methods could be used in whole flow field. More detail description of this method can be found in [11].

Numerical results

The code was tested for some laminar flow cases. The cases were chosen because they have been studied previously by others numerically or experimentally.

Driven cavity flow

Flow in 2–D square cavity provides a good test case if there no primary flow direction and the boundary conditions are very simple. This geometry has been used as a validation case by several authors [8, 21, 13, 18, 5] The above described method has been tested for a wide range of Reynolds numbers, Re with a polynomial degree of approximation up to seven. For Reynolds numbers up to 5000 the results practically coincide with data already published. Therefore we focus on a recently controversial case for $Re = 10000$.

For a long time the scientific discussion on the cavity flow for Reynolds number $Re = 10000$ was divided into two questions - is the flow field inside the cavity stationary or not. Some works report stable solutions until this value [8, 21, 15, 16]. But recent works [4, 5] assert, that the flow field is not stable at $Re = 10000$ and the first Hopf bifurcation occurs around $Re = 8000$. The calculations were performed on relatively dense computational grids 512×512 to 2048×2048 [5].

In the following section we present the results of the high order method but on much more sparse grids. In Fig.3 there is shown a plot of time series of velocity $\overline{v}_x$ inside a monitoring point for the grid 10×10 elements for a different degree of functional approximation. It is evident that for using the high degree orthonormal polynoms the solution is less damped and becomes periodical.

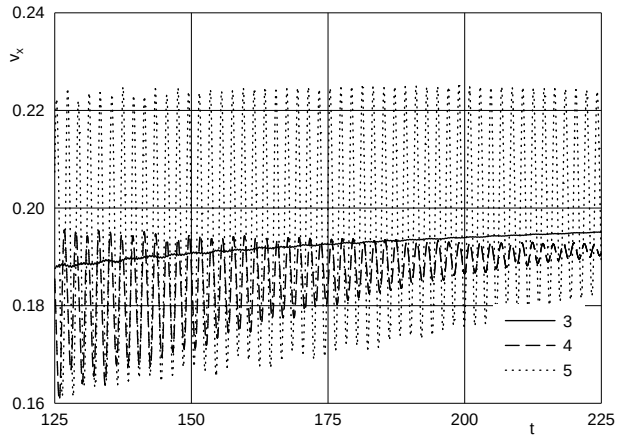

Figure 3: Horizontal velocity history at monitoring point (0.15,0.85). Rectangular cavity at $Re = 10000$. Grid 10×10, functional approximation degree 3 to 5.

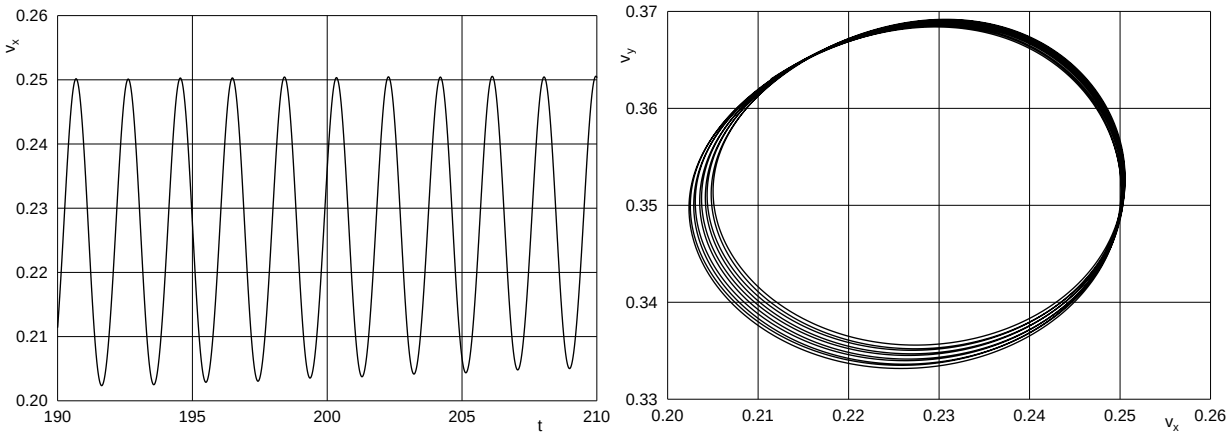

Figure 4: Horizontal velocity history and phase portrait at monitoring point (0.14,0.78). Rectangular cavity at $Re = 10000$. Grid 20×20, functional approximation degree 4.

If the grid is denser, say 20×20 elements, nearly steady periodical solution is obtained with orthogonal polynoms of four degree. The polynoms of higher order gives a very similar solution. It is clear that the high order functional approximation allows to describe an instability of flow field even for a very coarse grid of elements.

Flow over a circular cylinder

As an example of an external flow problem, the flow over 2–D circular cylinder was calculated. The code was run for inviscid and laminar–flow test cases.

The accuracy of the geometrical discretization and the efficiency of the solution are tested for the Euler equations of flow past a circular cylinder. A series of grids consisting of a different number of the triangular and isoparametric elements – linear or quadratic – have

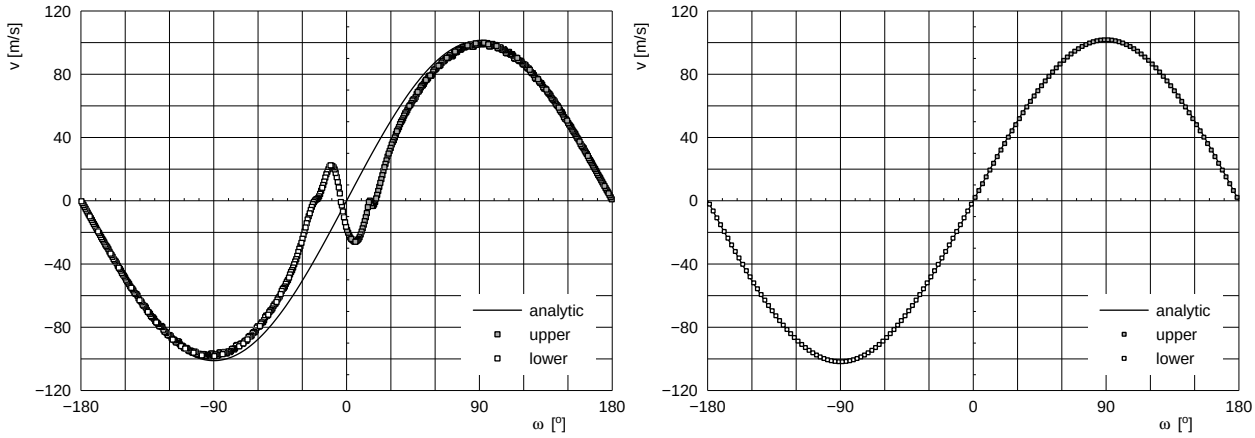

Figure 5: Euler equations of 2D flow past a circular cylinder. Linear approximation of a boundary (120 boundary elements, left) and quadratic approximation of a boundary (36 boundary elements, right).

been generated to study convergence of the discontinuous Galerkin method of various order.

The Riemann flux on cell boundaries is approximated by a simple and robust, but more dissipative, Lax–Friedrichs type flux [14, 22] of the form

$$\boldsymbol{F}^R(Q_i, Q_j) \circ \boldsymbol{n} = \frac{1}{2}[\boldsymbol{F}(Q_i) + \boldsymbol{F}(Q_j)] \circ \boldsymbol{n} - \frac{\lambda}{2}(Q_j - Q_i), \tag{17}$$

where λ is greater than a maximum of the absolutes of the eigenvalues of $\mathrm{d}\boldsymbol{F}/\mathrm{d}Q$. We can consider the second term of $\boldsymbol{F}^R$ approximation as a numerical viscosity, which is not present in Euler equations, but is required for the stability of numerical solution. Simultaneously there is necessity to reduce – as it is possible – an influence of this term in the solution.

As can be seen in Fig. 5, linear geometric approximation of a boundary leads to wrong artificial vortices downstream the cylinder even if a number of the boundary elements is relatively high. On the other hand the quadratic approximation provides good results even for a relatively low number of the boundary elements.

The above mentioned behaviour is intensified if the high order functional approximation is used. In such case the linear approximation of curved boundary can totally devalue the results. To successfully apply the high order functional approximation a high order approximation of the curved walls is required.

As an example of the solution of the Navier-Stokes equations a pressure field for $Re = 5$ is shown in Fig. 6. The calculated values of pressure coefficients c_p at the front and rear stagnation points are $c_{pf} = 1.88$ and $c_{pr} = -1.07$. Even if the coarser grid of 357 elements is used the results are well comparable with data in [7] ($c_{pf} = 1.872$ and $c_{pr} = -1.044$) and [19] ($c_{pf} = 1.847$ and $c_{pr} = -1.067$).

Another results that were obtained by this approach can be found in [9, 10] for Reynolds numbers up to 200000. The calculated flow field reasonably well correspond with available experimental data (e.g. [20]).

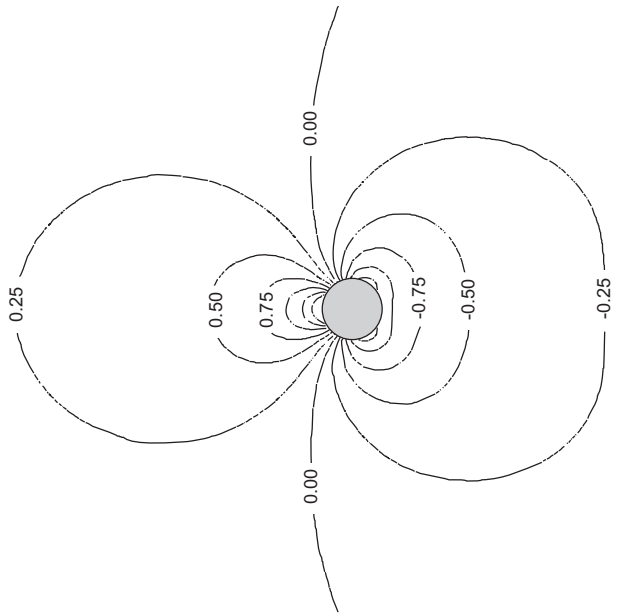

Figure 6: Pressure coefficient field $c_p = p - p_\infty / 0.5\rho V_\infty^2$ of 2D flow past a circular cylinder for $Re = 5$. Quadratic approximation of a boundary, orthonormal polynoms degree 4, mesh of 357 elements.

Conclusions

This paper shows that the application of the high order methods gives a very good results even on coarse grids. Another aspect is that the possibility to describe the flow instability more precisely was confirmed. This is very important for the numerical solution in a range of the Reynolds numbers when the transition from laminar to turbulent flow can occur.

Acknowledgements

The support under the project No.103/07/0136 of Grant Agency of the Czech Republic, and the Institutional Research Plan of IH ASCR AV0Z20600510 is gratefully acknowledged.

References

[1] D. A. Anderson, J. C. Tannehill, and R. H. Pletcher. *Computational fluid mechanics and heat transfer*. Hemisphere Publshing Corporation, New York, 1984.

[2] M. M. Athavale and C. L. Merkle. An upwind differencing scheme for time–accurate solutions of unsteady incompressible flow. *AIAA Paper*, 88(3650), 1988.

[3] H. L. Atkins and C.-W. Shu. Quadrature-free implementation of the discontinuous Galerkin method for hyperbolic equations. *AIAA Journal*, 36(5):775–782, 1997.

[4] F. Auteri, N. Parolini, and N. Quartapelle. Numerical investigation on the stability of singular driven cavity flow. *J. Comp. Phys.*, 183:1–25, 2002.

[5] C.-H. Bruneau and M. Saad. The 2D lid-driven cavity problem revisited. *Computers and fluids*, 35(3):326–348, 2005.

[6] A. J. Chorin. A numerical method for solving incompressible Navier–Stokes equations. *Journalof Computational Physics*, 2:12–26, 1967.

[7] S. C. R. Dennis and G. Z. Chang. Numerical solutions for steady flow past a circular cylinder at reynolds number up to 100. *J. Fluid Mech.*, 42:471–489, 1970.

[8] U. Ghia, K. N. Ghia, and C. T. Shin. High Re solutions for incompressible flow using the Navier–Stokes equations and a multigrid method. *J. Comp. Phys.*, 48:387–411, 1982.

[9] B. Horeni and Z. Chara. Numerical simulation of flow past circular cylinder for high subcritical reynolds numbers. In *XIX mezdunarodnaja naucnaja konferencija Matematiceskije metody v technike i technologijach MMTT-19, Voronez (RU)*, pages 82–85, 30.5–2.6 2006.

[10] B. Horeni and Z. Chara. Simulation of flow past circular cylinder for wide range of subritical reynolds numbers. In *Colloquium Fluid mechanics 2006, Praha (CZ)*, pages 61–64, 25–27.10. 2006.

[11] B. Horeni and Z. Chara. On fuid in a thin layer using discontinuous Galerkin method. *J. Hydrol. Hydromech.*, 55(1):24–42, 2007.

[12] M. A. Hulsen. The discontinuous Galerkin method with explicit Runge-Kutta time integration for hyperbolic and parabolic systems with source terms. Technical Report MEMT 19, Delft University of Technology, Laboratory for Aero and Hydrodynamics, Rotterdamseweg 145, 2628 AL Delft, The Netherlands, November 19, 1991.

[13] J. Kim and P. Moin. Application of fractional–step method to incompressible Navier–Stokes equations. *J. Comp. Phys.*, 59:308–323, 1985.

[14] R. J. LeVeque. *Finite Volume Methods for Hyperbolic Problems.* Cambridge University Press, Cambridge, 2002.

[15] M.Sahin and R. G. Owens. A novel fully–implicit finite volume method applied to lid–driven cavity problem, Part I: High reynolds number flow calculation. *Int. J. Numer. Methods Fluids*, 42(1):57–77, 2003.

[16] M.Sahin and R. G. Owens. A novel fully–implicit finite volume method applied to lid–driven cavity problem, Part II: Linear stability analysis. *Int. J. Numer. Methods Fluids*, 42(1):79–88, 2003.

[17] J. F. Remacle, J. E. Flaherty, and M. S. Shephard. An adaptive discontinuous Galerkin technique with an orthogonal basis applied to compressible flow problems. *SIAM Review*, 45(1):55–73, 2003.

[18] S. E. Rogers and D. Kwak. An upwind–differencing scheme for the incompressible Navier–Stokes equations. Technical Report TM–101051, NASA, November, 1988.

[19] S. E. Rogers and D. Kwak. An upwind differencing scheme for the time–accurate incompressible Navier–Stokes equations. *AIAA Paper*, 88(2583), 1988.

[20] H. Schlichting and K. Gersten. *Boundary-Layer Treory.* Springer Verlag, Berlin, 2003.

[21] R. Schreiber and H. B. Keller. Driven cavity flows by efficient numerical techniques. *J. Comp. Phys.*, 49:310–333, 1983.

[22] E. F. Toro. *Riemann Solvers and Numerical Methods.* Springer–Verlag, Berlin, 1997.